Solution study of the *Escherichia coli* DNA polymerase III clamp loader reveals the location of the dynamic ψχ heterodimer

Farzaneh Tondnevis,[1] Richard E. Gillilan,[2] Linda B. Bloom,[1] and Robert McKenna[1,a)]
[1]*Biochemistry and Molecular Biology, University of Florida, P.O. BOX 100245, Gainesville, Florida 32610, USA*
[2]*Cornell High Energy Synchrotron Source (CHESS), Cornell University, 161 Synchrotron Drive, Ithaca, New York 14853, USA*

(Received 1 May 2015; accepted 15 July 2015; published online 18 August 2015)

Several X-ray crystal structures of the *E. coli* core clamp loader containing the five core (δ', δ, and three truncated γ) subunits have been determined, but they lack the ψ and χ subunits. We report the first solution structure of the complete seven-subunit clamp loader complex using small angle X-ray scattering. This structure not only provides information about the location of the χ and ψ subunits but also provides a model of the dynamic nature of the clamp loader complex.
[http://dx.doi.org/10.1063/1.4927407]

I. INTRODUCTION

The rate of DNA synthesis in *E. coli* (∼1000 bp/s) is dependent on the function of the β sliding clamp and its associated clamp loader assembly.[1–3] The β sliding clamp is a homodimer ring-shaped protein[4] which confers processivity upon the replicative polymerase III and provides a mobile platform for interaction with various proteins during DNA damage repair, in addition to the polymerase.[5–8] The clamp loader complex is a member of the AAA+ family of ATPases (adenosine 5′-triphosphatases). The clamp loader utilizes ATP binding and hydrolysis to load the sliding clamp onto the DNA at the primer template junction[9–12] and is comprised of seven subunits (δ, 3τ or γ, δ', χ and ψ).[13–16] The δ subunit is responsible for clamp binding and opening. The δ' subunit acts as a stator and stabilizes the interaction of δ subunit with the sliding clamp.[17–20] The τ and γ subunits are the active ATPases, and both γ and τ are products of the *dnaX* gene.[21–23] The τ and γ clamp loading function is interchangeable and the major difference is in the length of the two proteins; γ is a shorter version of τ subunits that is created by a translational frame shift.[24,25] Each DnaX subunit (either τ or γ) binds one molecule of ATP, and the clamp loader binds and hydrolyses three ATP molecules for each loading cycle.[26]

The *E. coli* clamp loader complex contains two other subunits ψ and χ. These two subunits form a tight 1:1 elongated heterodimeric complex.[15,27] The ψ subunit interacts with the C-terminal region of γ subunit.[15,28] These two subunits are essential for bridging the interaction between the clamp loader and single strand DNA binding protein (SSB) in *E. coli*. The ψ subunit plays a role in stabilizing the conformational changes induced by ATP binding, the χ subunit directly interacts with the C terminus of SSB (8 amino acid residues), and the interaction of SSB with χ subunit is increased thousand of folds when SSB is bound to DNA.[29–31] The $\chi\psi$ complex also plays a role in increasing the affinity of τ and γ for $\delta.\delta'$ to a physiologically relevant range.[32]

a)Author to whom correspondence should be addressed. Electronic mail: rmckenna@ufl.edu Tel.: (352) 392-5696. Fax: 352-392-3422.

Several X-ray crystal structures of the *E. coli* clamp loader complex have been determined but all of these structures lack the ψ and χ subunits.[13,14,33] The X-ray crystal structure of the clamp loader complex bound to N-terminal 28 amino acids of ψ subunit[33] showed that this interaction is restricted to the collar region of the three DnaX (γ) subunits, and previous crosslinking studies have shown that the ψ subunit interacts with the γ subunit closest to the δ'.[29,34] Mass spectroscopy data have revealed a geometrical arrangement of the heterodimer where $\psi\chi$ extends over the two γ subunits and ψ adjacent to δ.[35] In these studies, we have obtained for the first time using small angle X-ray scattering a solution structure of the complete seven subunit *E. coli* clamp loader (δ, 3γ, δ', ψ and χ) complex in the presence of ATP. The Small Angle X-ray Scattering (SAXS) model reveals the location of the interaction of the χ and ψ subunit with the C-terminal region of the γ subunit away from the single stranded DNA exit site on δ subunit and closer to the δ' subunit in agreement with the crosslinking data. This structure also provides insight about the location of interaction of the $\chi\psi$ heterodimer with the clamp loader complex in the absence of DNA and provides possible mechanism for the interaction of the clamp loader complex with SSB.

II. MATERIAL AND METHODS

A. Protein expression and purification

The *E. coli* clamp loader complex subunits δ, γ, δ', χ, and ψ were expressed, purified, and reconstituted as described previously, and the clamp loader was reconstituted from purified subunits.[32,36–39] The storage buffer for γ complex contained: 20 mM Tris-HCl, 0.5 mM EDTA, 2 mM DTT, 10% glycerol, and 50 mM NaCl. The final ATP and $MgCl_2$ concentrations for clamp loader complex samples with ATP were 500 μM and 8 mM, respectively.

B. Small angle x-ray scattering

SAXS data (X-ray 9.881 keV, $\lambda = 1.256$ Å, (tantalum edge) at 1×10^{10} photons/s) were collected on the F2 station at the Cornell High Energy Synchrotron Source (CHESS) in Ithaca, New York. Prior to data collection, all samples were centrifuged at $15\,000 \times g$ for 10 min to remove any aggregates. For data collection, 30 μl of sample, which was in the storage buffer, was loaded manually and robotically oscillated in the beam. The storage buffer was used as buffer background (30 μl). The X-ray beam was collimated to 250×250 μm diameter and centered on a 2 mm diameter horizontal quartz capillary tube with 10 μm thick walls (Hampton Research, Aliso Viejo, CA). The capillary tube and full X-ray flight path, including beamstop, were kept *in vacuo* to eliminate air scatter. Data were captured on a Pilatus 100 K-S detector (Dectris, Baden, Switzerland) at 1500 mm distance. Scattering profiles were measured over the range of momentum transfer $0.01 < q = 4\pi \sin(\theta)/\lambda < 0.27$ Å^{-1}. The exposure time was 30 s, and 10 data sets were collected for possible radiation damage detection. Undamaged exposures were averaged and buffer subtracted using the RAW software.[40] Scattering data were also measured at different protein concentrations to check for presence of aggregation as a function of increasing concentration. For the clamp loader complex, the R_g values at varying concentrations (2.0, 1.0, 0.5, and 0.25 mg/ml) were 54.6 Å ± 1.4, 53.8 Å ± 1.0, 51.0 Å ± 1.3, and 54.3 Å ± 1.4. Data collection and scattering derived parameters are summarized in Table I.

C. Software and modelling of SAXS data

The ATSAS suite of programs (Hamburg, EMBL (European Molecular Biology Labs)) was used for data processing. The program PRIMUS was used to obtain the Guinier plot and to calculate the radius of gyration (R_g).[41] Linear fitting was performed on the data having $R_g.q < 1.3$ for Guinier analysis. The program GNOM[42] was used to calculate the particle distance distribution function P(r). The program DAMMIF (which is a rapid *ab initio* shape determination program using a single phase dummy sphere model)[43] was used to calculate the SAXS envelope by simulated annealing, and DAMMAVER was used to average the models.[44] Programs COOT[45] (crystallographic object oriented toolkit) and Chimera[46] were used to manually model

TABLE I. Data-collection and scattering-derived parameters Å.

	γ complex + ATP
Data-collection parameters	
Instrument	CHESS F2
Beam geometry	250 μm × 250 μm
Wavelength (Å)	1.256
q range ($Å^{-1}$)	0.01–0.27
Exposure time (s)	30
Concentration Range (mg/ml)	0.5–3.65
Temperature (K)	…
Structural parameters	
I(0) (cm^{-1}) [from P(r)]	4.80 ± 0.01
R_g(Å) [from P(r)]	54.7 ± 0.2
I(0) (cm^{-1}) [from Guinier]	4.77 ± 0.01
R_g(Å) [from Guinier]	53.4 ± 0.23
D_{max}(Å)	200
Software employed	
Primary data reduction	*RAW*
Data processing	*PRIMUS, SCATTER*
Ab initio analysis	*DAMMIF*
Validation and averaging	*DAMMAVER*
Rigid-body modeling	*COOT*
Computation of model intensities	*CRYSOL*
3D graphics representation	*CHIMERA, PyMOL*

the previously determined X-ray crystal structures of the *E. coli* δ, 3γ, δ' (PDB: 3GLF)[33] complex (with the additionally modelled DnaX regions (369–431)) and heterodimeric χ and ψ complex (PDB:1EM8)[16] into the clamp loader SAX envelope. Chimera was then used to rigid body fit the individual protein subunits into the SAX envelope. The program CRYSOL[47] was used to calculate theoretical scattering curves for comparison of the clamp loader complex crystal models and the experimental 1D scattering curve.

III. RESULTS

A. 1D scattering curve, shape, and quality characterization

We obtained SAXS profiles for the complete clamp loader complex. The 1D scattering curve for the clamp loader complex in the presence of 500 μM ATP is shown (Fig. 1(a)). The Guinier analysis of the scattering curve (which is analysis of the scattering curve at very low angles, or small q values) is shown (Fig. 1(b)). The Guinier plot shows no deviation from linearity, and the linearity is consistent with the sample being monodisperse. The $R_g.q < 1.3$ requirement for the globular proteins was satisfied. The radius of gyration R_g, which provides information about the rotational volume of the macromolecule, was calculated to be 55.4 ± 0.3 Å (sample at 3.7 mg/ml). The consistency of R_g values at different concentrations, list in material and methods section, indicates that there were no concentration effects.

The pair distance distribution function, denoted as P(r), was calculated using the inverse Fourier method as implemented in the GNOM[42] program. In SAXS, the P(r) function is used to describe the paired-set of distances between all of the points within the macromolecular structure and is a useful tool for predicting the overall shape of the molecule as well as visibly detecting conformational changes within a macromolecule. The P(r) function curve for the clamp loader complex in Fig. 1(c) shows that the clamp loader complex is generally spherical in shape (the bell shape curve is centered around 65 Å with additional extended domains as

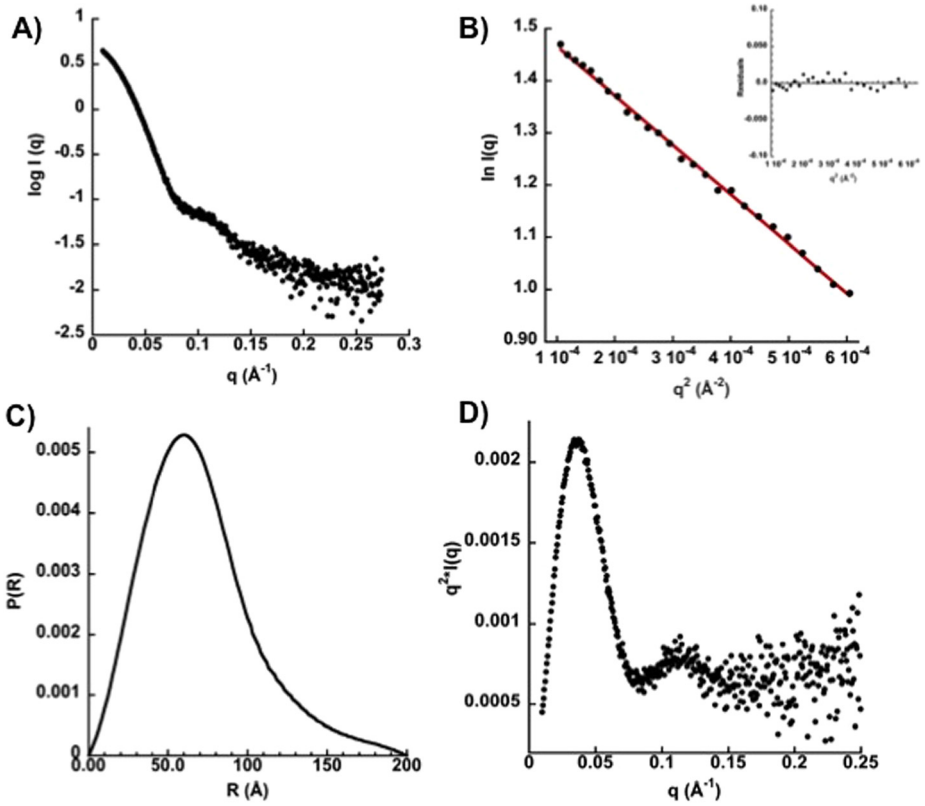

FIG. 1. SAXS data of the clamp loader complex in the presence of ATP. (a) 1D scattering curve. The curve shown is the average of 10 data sets and buffer subtracted. (b) Guinier analysis of the clamp loader. The R^2 value for the line was 0.998. The inset is the residual of the Guinier curve linear fit in $R_g.q < 1.3$ region. (c) The pair wise distance distribution function curve of the clamp loader complex reveals a protein with an extended domain. The D_{max} was 200 Å. (d) The Kratky plot of the clamp loader complex calculated using SASPLOT.

depicted by the presence of the tail at larger distances). The D_{max} value was determined to be 200 Å. The D_{max} calculated for the crystal structure of seven subunit clamp loader core complex later shown in Fig. 2(d) was roughly 190 Å. The slightly larger D_{max} is expected due to the hydration shell that is absent from the crystal structures of the clamp loader complex and flexibility of the clamp loader in solution. The fit of the P(r) curve to the 1D scattering curve is also shown.[50] To ensure that the protein was folded properly, we generated the Kratky plot using the SASPLOT software (feature of PRIMUS). The Krakty plot for the clamp loader complex in the presence of ATP is shown (Fig. 1(d)). The plot shows the presence of a bell shape peak and convergence to x-axis at higher q values expected from a folded globular protein.

B. SAXS *ab initio* and rigid body modelling

To obtain three-dimensional molecular envelopes of the clamp loader complex, the program DAMMIF[43] was used. P1 symmetry was imposed for model prediction, ten models were generated for the clamp loader (at 3.7 mg/ml),[50] and the program DAMAVER[44] was used to find the reference model, align all the models with the reference model, and average the dummy sphere models. The mean normalized special discrepancy (NSD) value, which provides agreement between the SAXS envelopes, for individual clamp loader complex bound to ATP was 0.49 ± 0.016. The NSD values below 1 are acceptable, values between 0.5 and 0.7 reflect a good model, and a value below 0.5 is an excellent model. The predicted solution structure (the average of these ten models) for γ complex clamp loader bound in presence of ATP is shown (Fig. 2(a)). The central primer template-binding cavity as well as the region in the δ subunit where the single strand DNA branches away is highlighted in Fig. 2(a). When compared to the

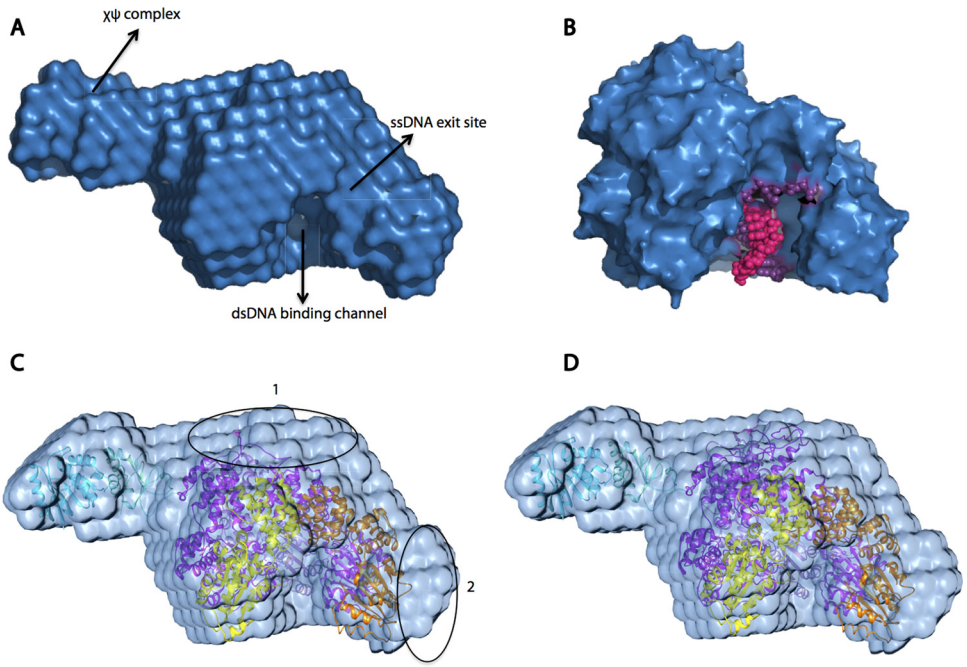

FIG. 2. SAXS model of the clamp loader complex in the presence of ATP. (a) The SAXS envelope of the clamp loader complex (average of 10 models). The 3D model was generated using the DAMMIF *ab initio* shape determination software and averaged by DAMMAVER. The location of $\chi\psi$ heterodimer, as well as the dsDNA central cavity and ssDNA exit channel on the δ subunit, is marked by arrows. (b) The surface representation of the crystal structure of the heteropentameric clamp loader complex (blue) bound to primer template DNA (light and dark pink) (PDB: 3GLF) is shown for comparison with the SAXS model. (c) Fit of the crystal structures of the δ, 3γ, δ', χ, and ψ (δ: orange, γ: shades of purple, δ': yellow, χ: cyan, and ψ: aquamarine) into the SAXS envelope. The extra density for the C-terminal regions of the 3γ subunits and the density for the δ subunits are numbered as 1 and 2, respectively. (d) Fit of the crystal structure as in C except for addition of modelled C-terminal missing residues (370–431) on 3γ subunits. The correlation coefficient of the fit in D was 0.9.

previously determined X-ray crystal structure of the clamp loader complex comprised of the five core subunits (PDB: 3GLF)[33] (Fig. 2(b)), there is extra density forming an "arm" on the surface of the five-subunit core that is not present in the surface representation of the crystal structure of δ, 3γ, and δ' complex bound to DNA. This density most likely corresponds to the χ and ψ heterodimeric complex that is absent in all the crystal structures of the *E. coli* clamp loader complex previously determined.

The C-terminal regions of the γ subunits (residues 374–431) are truncated in the crystal structures because of the flexibility of this region. In the X-ray crystal structures, residues 374–431 of the 3γ subunits are cleaved by protease treatment or use of truncated protein (residues 1–373).[14,33,48] The extra density is large enough in volume to accommodate the missing flexible regions of the three γ subunits (marked 1 in Fig. 1(c)) but too small for accommodating the ψ and χ subunits, and therefore, we modelled as the truncated C-terminal regions of the three γ subunits and the extra density opposite the δ subunit to χ and ψ. Once the seven-subunit clamp loader model was docked into the SAXS envelope, it was discovered that there is a second region of extra density in the envelope as shown (marked 2 in Fig. 1(c)) which we believe indicates movement of the δ subunit possibly in readiness for binding the β sliding clamp and is not captured in crystal structures possibly because of crystal packing effects. A crystal-packing diagram for the γ-clamp loader is shown.[50]

To check the validity of this SAXS envelope, the seven-subunit clamp loader complex (as shown in Fig. 2(c)) was docked into the SAXS 3D envelope and energy minimized using CHIMERA.[46] In addition, we generated a 3D model for the region of the γ subunit that was truncated for crystallography (374–431) using the Robetta server from Baker's lab,[49] and this structure was merged onto the three γ subunits (Fig. 2(d)). The correlation coefficient value for

this docking was 0.9, which indicates a good fit of the crystal structure into the SAXS envelope. The ψ subunit was modelled to interact with the C-terminal collar region of the γ subunit next to δ', based on the previous knowledge of ψ interacting with the clamp loader and χ interacting with SSB.

For comparing the SAXS experimental scattering data to the atomic crystal structure models of the clamp loader complex, CRYSOL[47] was used. Three theoretical scattering curves were generated as shown (Fig. 3). The blue curve is the predicted curve for the five-subunit clamp loader complex using the PDB: 3GLF.[33] The χ value was 5.6, and theoretical R_g value was 45.5 Å. The green curve is the predicted scattering curve for the seven subunit clamp loader complex as shown in Fig. 1(d) with $\psi\chi$ modeled close to the δ' subunit based on *ab inito* SAXS structure with χ value of 2.2. The red curve is the predicted scattering curve for the seven-subunit clamp loader complex with $\psi\chi$ subunits positioned close to the ssDNA exit channel on the δ subunit with χ value of 4.2 and theoretical R_g value of 46.8 Å. It is evident from CRYSOL analysis that the predicted curve of the five subunit clamp loader complex in the absence of $\psi\chi$ heterodimer does not fit scattering curve at low and high q values and having the χ value of 5.6 and R_g value of 45.5 Å. The CYROSL predicted curve for the seven-subunit clamp loader complex with $\psi\chi$ positioned close to δ' subunit has the best fit to experimental data as evident by the lowest χ value and better fit to the experimental data as well as better agreement of theoretical R_g value of 51.1 Å with the experimental R_g value of 53.4 Å. The discrepancy between the theoretical scattering curves for the seven subunit clamp loaders (red and green curve) and the experimental data at $q = 0.125\ Å^{-1}$ could possibly be the result of the intramolecular movement or "breathing" of the clamp loader subunits in solution that are otherwise absent from static state X-ray structures.

III. DISCUSSION

The *E. coli* clamp loader complex is a member of the AAA+ family of ATPases and is comprised of seven subunits (δ, δ', 3γ or τ, ψ and χ). Each of these has critical roles in the function of the clamp loader. The three γ or τ subunits are the active ATPases, and each binds one molecule of ATP. The δ subunit binds and opens the sliding clamp, and the δ' subunit stabilizes

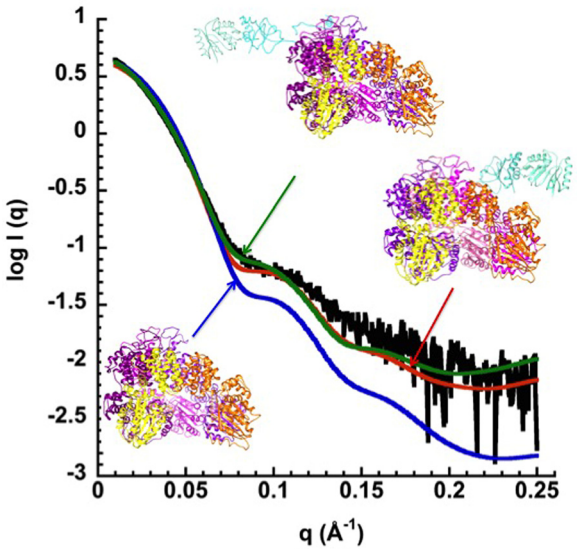

FIG. 3. Comparison of the solution scattering data and CRYSOL predicted curves. The γ-clamp loader complex SAXS scattering data are shown in black. The CRYSOL[47] theoretical scattering curve calculated for five-core subunit clamp loader without $\chi\psi$ subunits (PDB: 3GLF) is shown in blue ($\chi = 5.6$). The CRYSOL theoretical predicted curve calculated for seven-subunit clamp loader complex with $\chi\psi$ subunits positioned close to ssDNA exit channel on δ subunit is shown in red ($\chi = 4.2$) and theoretical curve calculated for seven-subunit clamp loader complex with $\chi\psi$ subunits positioned close to the δ' subunit is shown in green with the χ value of 2.2.

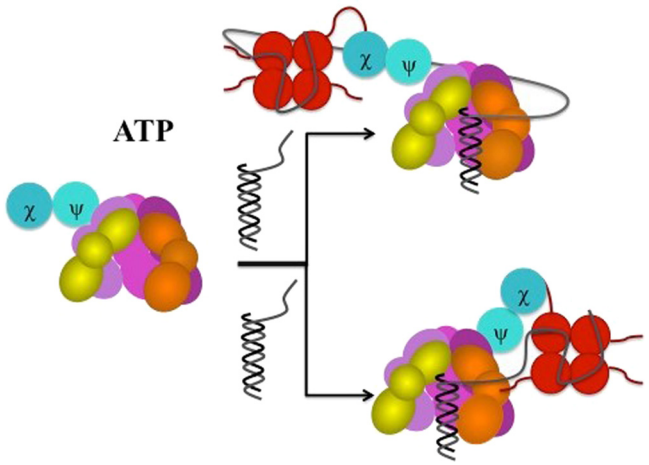

FIG. 4. Model of the clamp loader-SSB interaction. The clamp loader subunits color-coding is as follows: δ: orange, γ: shades of purple, δ': yellow, χ: cyan, and ψ: aquamarine SSB monomeric units in red, and SSB monomers C-terminal tails in dark red. The primer template DNA is shown in shades of grey. The clamp loader when bound to ATP is in a favorable conformation for interaction with the sliding clamp and the DNA. When bound to primer template DNA, the ssDNA exiting the ssDNA exit channel on the δ' subunit can either wrap around the clamp loader complex or the $\chi\psi$ heterodimer can rotate (because of the flexible N-terminal poly peptide on ψ) and bring the SSB closer to the δ subunit for interaction with the ssDNA.

the interaction of the δ subunit with the clamp, while the χ and ψ subunits bridge the clamp loader complex with the SSB. The ψ N-terminal 28 amino acids are responsible for anchoring the $\psi\chi$ to the clamp loader complex.[16,33] The crystal structure of the clamp loader complex with the five core subunits in the presence of the ψ peptide (residues 2–28) has been determined.[33] The X-ray crystal structure and biochemical studies of the clamp loader complex bound to the ψ peptide showed that this interaction is restricted to the collar region of the three DnaX subunits,[29] but, to this date, there has been no cryo-EM, X-ray, or SAXS structure of the *E. coli* seven subunit clamp loader complex. In these studies, we have obtained for the first time a low resolution SAXS model of the complete (all seven subunits) gamma clamp loader complex in the presence of ATP. The SAXS envelope suggests that the ψ and χ subunits mainly interact in an asymmetrical fashion with the collar C-terminal region of one of the γ subunits (the γ subunit next to δ') (Fig. 2(a)), which is consistent with the previous crosslinking studies showing that the ψ subunit interacts with the γ subunit closest to the δ'.[29,34] This finding has implication that there is possible wrapping of ssDNA around the collar region for interaction with SSB at the replication fork (Fig. 4). The second possibility is that upon interaction of the clamp loader complex with the DNA, there is movement of $\psi\chi$ possibly through the flexible N-terminal region of ψ, so that the SSB is located closer to the ssDNA exit channel on the δ subunit and this second model is in agreement with ion mobility mass spectroscopy data.[35] It should be noted that the solution structure of the clamp loader complex discussed in this paper could possibly describe one of the several conformations of an ensemble of conformations expected of a highly dynamic macromolecule such as the clamp loader complex and that there might be a switching mechanism between the active and inactive state of the clamp loader upon binding of the DNA. The clamp loader complex SAXS model also reveals that the δ subunit possibly undergoes some movements to be able to make contact with the β sliding clamp to open or to stabilize an open clamp and that the additional envelope volume highlighted in Fig. 2(c) is indicative of the location of the δ subunit in readiness to bind the clamp. These dynamics could not have been captured in previously determined solid-state X-ray crystal structures.

ACKNOWLEDGMENTS

This work was based upon research conducted at the Cornell High Energy Synchrotron Source (CHESS), which is supported by the National Science Foundation and the National Institutes of

Health/National Institute of General Medical Sciences under NSF Award DMR-0936384, using the Macromolecular Diffraction at CHESS (MacCHESS) facility, which is supported by award GM-103485 from the National Institute of General Medical Sciences, National Institutes of Health. This work was also supported by the NIH T32 training Grant No. 2T32AI007110-31A1.

[1]C. S. McHenry, Annu. Rev. Biochem **80**, 403 (2011).
[2]A. Johnson and M. O'Donnell, Annu. Rev. Biochem **74**, 283 (2005).
[3]J. Hurwitz and S. Wickner, Proc. Natl. Acad. Sci. USA **71**, 6 (1974).
[4]X. P. Kong, R. Onrust, M. O'Donnell, and J. Kuriyan, Cell **69**, 425 (1992).
[5]C. Indiani, P. McInerney, R. Georgescu, M. F. Goodman, and M. O'Donnell, Mol. Cell **19**, 805 (2005).
[6]V. Pages and R. Fuchs, Oncogene **21**, 8957 (2002).
[7]G. Maga and U. Hübscher, J. Cell Science **116**, 3051 (2003).
[8]J. B. Vivona and Z. Kelman, FEBS Lett. **546**, 167 (2003).
[9]A. F. Neuwald, L. Aravind, J. L. Spouge, and E. V. Koonin, Genome Res **9**, 27 (1999), http://www.ncbi.nlm.nih.gov/pubmed/9927482.
[10]T. Ogura and A. J. Wilkinson, Genes Cells **6**, 575 (2001).
[11]P. I. Hanson and S. W. Whiteheart, Nat. Rev. Mol. Cell Biol. **6**, 519 (2005).
[12]L. M. Iyer, D. D. Leipe, E. V. Koonin, and L. J. Aravind, Struct. Biol. **146**, 11 (2004).
[13]S. L. Kazmirski, M. Podobnik, T. F. Weitze, M. O'Donnell, and J. Kuriyan, Proc. Natl. Acad. Sci. U.S.A. **101**, 16750 (2004).
[14]D. Jeruzalmi, M. O'Donnell, and J. Kuriyan, Cell **106**, 429 (2001).
[15]H. Xiao, Z. Dong, and M. O'Donnell, J. Biol. Chem. **268**, 11773 (1993).
[16]J. M. Gulbis, S. L. Kazmirski, J. Finkelstein, Z. Kelman, M. O'Donnell, and J. Kuriyan, Eur. J. Biochem **271**, 439 (2004).
[17]R. Onrust and M. O'Donnell, J. Biol. Chem **268**, 11766 (1993), http://www.ncbi.nlm.nih.gov/pubmed/8505304.
[18]B. Stillman, Cell **78**, 725 (1994).
[19]B. Guenther, R. Onrust, A. Sali, M. O'Donnell, and J. Kuriyan, Cell **91**, 335 (1997).
[20]T. Oyama, Y. Ishino, I. Cann, S. Ishino, and K. Morikawa, Mol. Cell **8**, 455 (2001).
[21]M. O'Donnell, R. Onrust, F. B. Dean, and M. Chen, Nucl. Acids Res. **21**, 1 (1993).
[22]A. Blinkova, C. Hervas, P. T. Stukenberg, R. Onrust, M. O'Donnell, and J. R. Walker, J. Bacteriol. **175**, 6018 (1993), http://www.ncbi.nlm.nih.gov/pubmed/8376347.
[23]S. H. Lee, P. Kanda, R. C. Kennedy, and J. R. Walker, Nucl. Acids Res. **15**, 7663 (1987).
[24]A. M. Flower and C. S. McHenry, Nucl. Acids Res. **14**, 8091 (1986).
[25]A. M. Flower and C. S. McHenry, Proc. Natl. Acad. Sci. U.S.A. **87**, 3713 (1990).
[26]Z. Tsuchihashi and A. Kornberg, J. Biol. Chem. **264**, 17790 (1989), http://www.ncbi.nlm.nih.gov/pubmed/2681183.
[27]M. O'Donnell and P. S. Studwell, J. Biol. Chem. **265**, 1179 (1990), http://www.ncbi.nlm.nih.gov/pubmed/2404006.
[28]D. X. Gao and C. S. McHenry, J. Biol. Chem. **276**, 4447 (2001).
[29]B. P. Glover and C. S. McHenry, J. Biol. Chem. **273**, 23476 (1998).
[30]Z. Kelman, A. Yuzhakov, and J. Andjelkovic, EMBO J. **17**, 2436 (1998).
[31]G. Witte, C. Urbanke, and U. Curth, Nucl. Acids Res. **31**, 4434 (2003).
[32]M. W. Olson, H. G. Dallmann, and C. S. McHenry, J. Biol. Chem. **270**, 29570 (1995).
[33]K. R. Simonetta, S. L. Kazmirski, E. R. Goedken, A. J. Cantor, B. A. Kelch, R. McNally, S. N. Seyedin, D. L. Makino, M. O'Donnell, and J. Kuriyan, Cell **137**, 659 (2009).
[34]B. P. Glover and C. S. McHenry, J. Biol. Chem. **275**, 3017 (2000).
[35]A. Politis, A. Y. Park, Z. Hall, and B. T. Ruotolo, J. Mol. Biol. **425**, 4790 (2013).
[36]S. G. Anderson, C. R. Williams, M. O'Donnell, and L. B. Bloom, J. Biol. Chem. **282**, 7035 (2007).
[37]R. Onrust, J. Finkelstein, V. Naktinis, J. Turner, L. Fang, and M. O'Donnell, J. Biol. Chem. **270**, 13348 (1995).
[38]Z. Dong, R. Onrust, M. Skangalis, and M. O'Donnell, J. Biol. Chem. **268**, 11758 (1993), http://www.ncbi.nlm.nih.gov/pubmed/8505303.
[39]H. Maki and A. Kornberg, J. Biol. Chem. **260**, 12987 (1985), http://www.ncbi.nlm.nih.gov/pubmed/2997151.
[40]S. S. Nielsen, M. Moller, and R. E. Gillilan, J. Appl. Crystallogr. **45**, 213 (2012).
[41]P. V. Konarev, V. V. Volkov, A. V. Sokolova, M. H. J. Koch, and D. I. Svergun, J. Appl. Crystallogr. **36**, 1277 (2003).
[42]D. I. Svergun, J. Appl. Crystallogr. **25**, 495 (1992).
[43]D. Franke and D. I. Svergun, J. Appl. Crystallogr. **42**, 342 (2009).
[44]V. V. Volkov and D. I. Svergun, J. Appl. Crystallogr. **36**, 860 (2003).
[45]P. Emsley and K. Cowtan, Acta Crystallogr. D **60**, 2126 (2004).
[46]E. F. Pettersen, T. D. Goddard, C. C. Huang, G. S. Couch, D. M. Greenblatt, E. C. Meng, and T. E. Ferrin, J. Comput. Chem. **25**, 1605 (2004).
[47]D. Svergun, C. Barberato, and M. Koch, J. Appl. Cryst. **28**, 768 (1995).
[48]S. L. Kazmirski, Y. Zhao, G. D. Bowman, M. O'Donnell, and J. Kuriyan, Proc. Natl. Acad. Sci. U.S.A. **102**, 13801 (2005).
[49]K. T. Simons, C. Kooperberg, E. Huang, and D. Baker, J. Mol. Biol. **268**, 209 (1997).
[50]See supplementary material at http://dx.doi.org/10.1063/1.4927407 for fit of P(r) curve to 1D experimental cure, individual *ab initio* models, and diagram of crystal packing effects.